Supendi *et al. Geosci. Lett.* (2019) 6:18
https://doi.org/10.1186/s40562-019-0148-9

Geoscience Letters

RESEARCH LETTER Open Access

Hypocenter relocation of the aftershocks of the Mw 7.5 Palu earthquake (September 28, 2018) and swarm earthquakes of Mamasa, Sulawesi, Indonesia, using the BMKG network data

Pepen Supendi[1,2,4*], Andri Dian Nugraha[3,4], Sri Widiyantoro[3,4], Chalid Idham Abdullah[5], Nanang T. Puspito[3,4], Kadek Hendrawan Palgunadi[6], D. Daryono[7] and Samsul Hadi Wiyono[7]

Abstract

On September 28, 2018, the Mw 7.5 earthquake occurred in Palu, Central Sulawesi, Indonesia. This earthquake produced strong tremors, landslides, liquefaction and a tsunami and caused thousands of fatalities and damaged houses and infrastructure. We have relocated 386 of the 554 Palu aftershocks by using the double-difference relocation method (hypoDD) from September 28 to November 22, 2018. The aftershock pattern is consistent with the crustal deformation in the area and generally shows that the events have a NW–SE trending of ~ 200 km in length and ~ 50 km in width. Most of the aftershocks are located to the east of the Palu-Koro Fault Line. Since November 2, 2018, there have been hundreds of swarm earthquakes in the area of Mamasa, West Sulawesi, which is about 230 km south of the city of Palu. Some of these earthquakes were felt, and houses were even damaged. We have relocated 535 of the 556 swarm earthquakes having a magnitude of *M* 2 to *M* 5.4. Our results show that the seismicity pattern has a dip that becomes shallower to the west (dipping at a ~ 45° angle) and extends from north to south for a length of ~ 50 km. We also conducted a focal mechanism analysis to estimate the type of fault slip for selected events of an *M* > 4.5 magnitude. Most of the solutions of the focal mechanism analysis show a normal fault type. This swarm earthquake probably corresponds to the activity of the fault in the local area.

Keywords: Aftershocks, Palu, Swarm earthquakes, Mamasa, Double-difference

Introduction

On September 28, 2018, an Mw 7.5 devastating earthquake and tsunami affected the city of Palu in Central Sulawesi, Indonesia. As of November 22, 2018, the Indonesian Agency for Meteorology, Climatology, and Geophysics (BMKG) has recorded 554 aftershocks in this area with a significant number of events having a magnitude ≥ 3 with the use of a dense regional seismic network. According to the BMKG catalog, the mainshock occurred at 10:02:44 UTC and the epicenter was located at 0.18° S; 119.85° E with a depth of 10 km depth (Fig. 1). About 12 min after the mainshock, a sequence of aftershocks continued occurring until the final date that these data were downloaded, which was November 23, 2018, but even after that aftershocks still occurred. The shake map from BMKG and the community reports indicate that the earthquake was rated VII to VIII on the Modified

*Correspondence: pepen_geophysics@yahoo.com
[1] Geophysical Engineering Study Program, Faculty of Mining and Petroleum Engineering, Institut Teknologi Bandung, Bandung 40132, Indonesia
Full list of author information is available at the end of the article

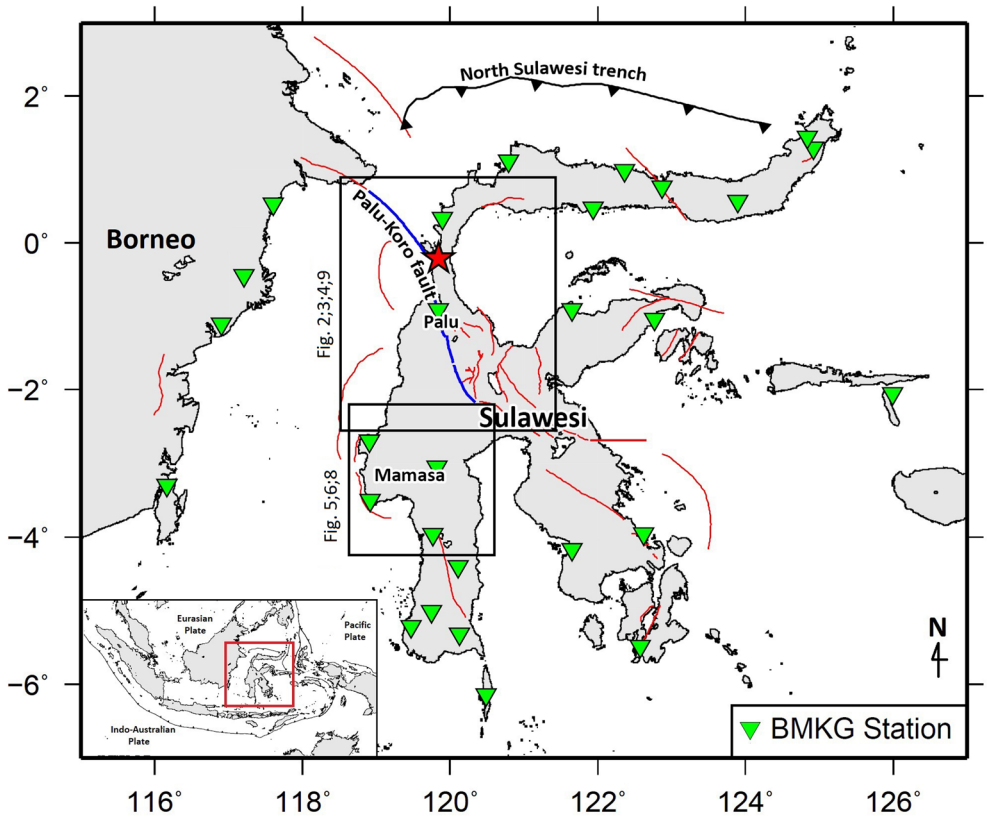

Fig. 1 Map of the study area. The red star depicts the Mw 7.5 mainshock; the green inverted triangles are the BMKG seismic station used in this study; blue traces represent the Palu-Koro Fault; and red traces correspond to the other major crustal faults in the region extracted from Irsyam et al. (2017). The black boxes show the map regions of Figs. 2, 3, 4, 5, 6, 8 and 9

Mercalli Intensity (MMI) scale in Palu and the surrounding area.

According to the National Disaster Management Authority (NDMA) report (http://bnpb.go.id/en), the tsunami and liquefaction caused more than 4000 fatalities. The geological map made by Watkinson (2011) shows that the city of Palu consists of Holocene sedimentary rock. Pramono et al. (2017) used the multichannel analysis of surface waves (MASW) method to conclude that the city of Palu and its surrounding area consist of alluvium and soft soil. Thus, the damage caused by the earthquake and the liquefaction was massive in the Palu area. Gusman et al. (2019) showed that the tsunami was caused by a combination of sudden ground and seafloor changes due to the earthquake, along with landslides, and a high tide at the time of the event.

The earthquake was generated by the strike-slip faulting of the Palu-Koro Fault (Bao et al. 2019; Socquet et al. 2019). The Palu-Koro Fault has a slip rate of about 42 mm/year, which was estimated by Global Positioning System (GPS) and slip rate modeling (Socquet et al. 2006). Daryono (2016) suggested that this fault includes active faults with a slip rate of around 30–40 mm yearly and can potentially generate a co-seismic slip. As a result, seismic hazard along Palu-Koro Fault segment in the vicinity of a highly populated area is also increasing.

Interestingly, a month after the mainshock, a swarm earthquake occurred in Mamasa, which is ~ 230 km to the south of Palu (Fig. 1). As of November 22, 2018, the BMKG has recorded 556 events with a magnitude of $M > 2$. These were located in the area at an average depth of 10 km. Unfortunately, some of the earthquakes caused damage to several houses and economic loss. However, the source of these swarm earthquakes is still unclear: whether they occurred due to known activity at currently dormant volcanoes or a static triggering as a result of the devastating Palu earthquake. Therefore, this study aims to relocate the aftershocks of the Palu earthquake and the swarm earthquakes to obtain more precise hypocenter locations, as well as to conduct a focal mechanism analysis to estimate the fault type in the Mamasa area.

Data and method

The arrival time data used in this study were obtained from September 28 to November 22, 2018, at BMKG seismic stations in Sulawesi and Borneo (Fig. 1). During this period, there were 554 aftershocks from the Palu earthquake and 556 swarm earthquakes from Mamasa, constituting 5608 and 2649 P- and S-wave arrival times, respectively. The velocity model from IASPEI91 (Kennett and Engdahl 1991) was used for the initial hypocenter determination of the BMKG catalog, using the SeisComP3 program (GFZ).

We used the HypoDD program (Waldhauser 2001) to perform the double-difference method (Waldhauser and Ellsworth 2000) for relocating the aftershock hypocenters. The method assumes that if there are two earthquakes with a hypocentral distance smaller than the distance from the hypocenters to the station, then the ray paths of these two earthquakes to the station can be assumed to be the same and therefore, propagate through the same medium. This method has been successful in relocating earthquakes in Indonesia using the BMKG network data with some prominent tectonic interpretations: for example, in Sumatra (Nugraha et al. 2018a), West Java (Supendi et al. 2018a), Sulawesi (Ismullah et al. 2017; Supendi et al. 2018b) and Molucca (Utama et al. 2015; Nugraha et al. 2018b).

We applied a statistical resampling approach "bootstrap" method (Efron 1982; Billings 1994; Shearer 1997) to assess the reliability of the error estimates. For the final hypocenters, we replaced the final residuals with samples drawn with replacements from the observed residual distribution and relocated all events with these bootstrap sample data and unit weights to determine the shift in location with the resampled data vector. We applied Gaussian noise to the data with a standard deviation 0.1 s. The process was then repeated 1000 times.

For selected events in the Mamasa earthquakes, we used the ISOLA package (Sokos and Zahradnik 2008) to perform moment tensor inversions from at least four BMKG seismic stations (see inverted green triangles in Fig. 1). The observed waveforms were preprocessed using a high-pass filter with a corner frequency of 0.075 Hz to 0.15 Hz. For hypocenter relocation and focal mechanism determination, we used the 1-D seismic velocity model AK135 (Kennett et al. 1995).

Results and discussion

We have relocated 386 aftershocks from the Palu earthquake (Fig. 2). We first compared the relocated aftershocks with the initial locations (Fig. 3). The relocated hypocenters were then plotted in the vertical cross section and show a northwest–southeast trending (Fig. 3). The relocated hypocenters exhibit an improvement in clustering both horizontally and vertically, as shown in Fig. 3. Relative location errors for the 386 aftershocks along the Palu-Koro Fault are shown in Fig. 4. Relative horizontal and vertical error ellipses are shown to be at the 95% confidence level. Ellipses are computed from the major axes of the horizontal and vertical projection of the 95% confidence ellipsoids obtained from a bootstrap analysis of the final double-difference vector. The distribution of the major and minor axes of the horizontal and vertical projections of the ellipsoids for the Palu aftershocks is shown in Fig. 7a. Average mislocations horizontally and vertically are generally less than 2 km, and the maximum dislocation is less than 13 km (Table 1).

The distribution of aftershocks extended from the north to the south of the mainshock (Fig. 2). The location of the aftershocks is consistent with the crustal deformation data in the area. The Geospatial Information Authority of Japan (GSI) applied interferometric analysis using ALOS-2/PALSAR-2 data to show that crustal deformation occurred in the part of the island (https://www.gsi.go.jp). Based on the vertical cross section in parallel to the fault (cross section A), the aftershocks were mostly located less than a depth of 20 km, which stay within the seismogenic zone, whereas the trend shown by the hypocenter in the northern part (close to the Mw 7.5 mainshock) is shallower than in the southern part. Based on the distribution of relocated aftershocks, it can be seen that the events have a NW–SE trending about ~ 200 km in length and ~ 50 km in width.

We have relocated 535 of the 556 swarm earthquakes in Mamasa with a magnitude of M 2 to M 5.4 (Fig. 5). The events that had previously been held fixed at 10 km could now be relocated/resolved (Fig. 5). Our results show that the earthquake swarms probably correspond to the activity of the local fault in the area, indicated by the fact that the seismicity pattern has a dip that becomes shallower toward the west (dipping at a ~ 45° angle) and extends from north to south with a length of ~ 50 km (Fig. 8b). Relative location errors for the 535 swarm earthquakes in Mamasa are shown in Fig. 6. The distribution of the major and minor axes of the horizontal and vertical projections of these ellipsoids for the events is shown in Fig. 7b. The spatial distribution of relative error agrees with the relocated seismicity pattern. This confirms that the seismic swarm sequence has a dip with a 45° angle. Average mislocations horizontally and vertically are less than 1.1 km, and the maximum dislocation is less than 9 km (Table 2).

We also conducted a focal mechanism analysis to estimate the type of fault slip for selected events with a magnitude of $M > 4.5$ (Fig. 8a). Most of the focal mechanism solutions show the normal fault type. We plotted a spatiotemporal distribution of the aftershocks right after

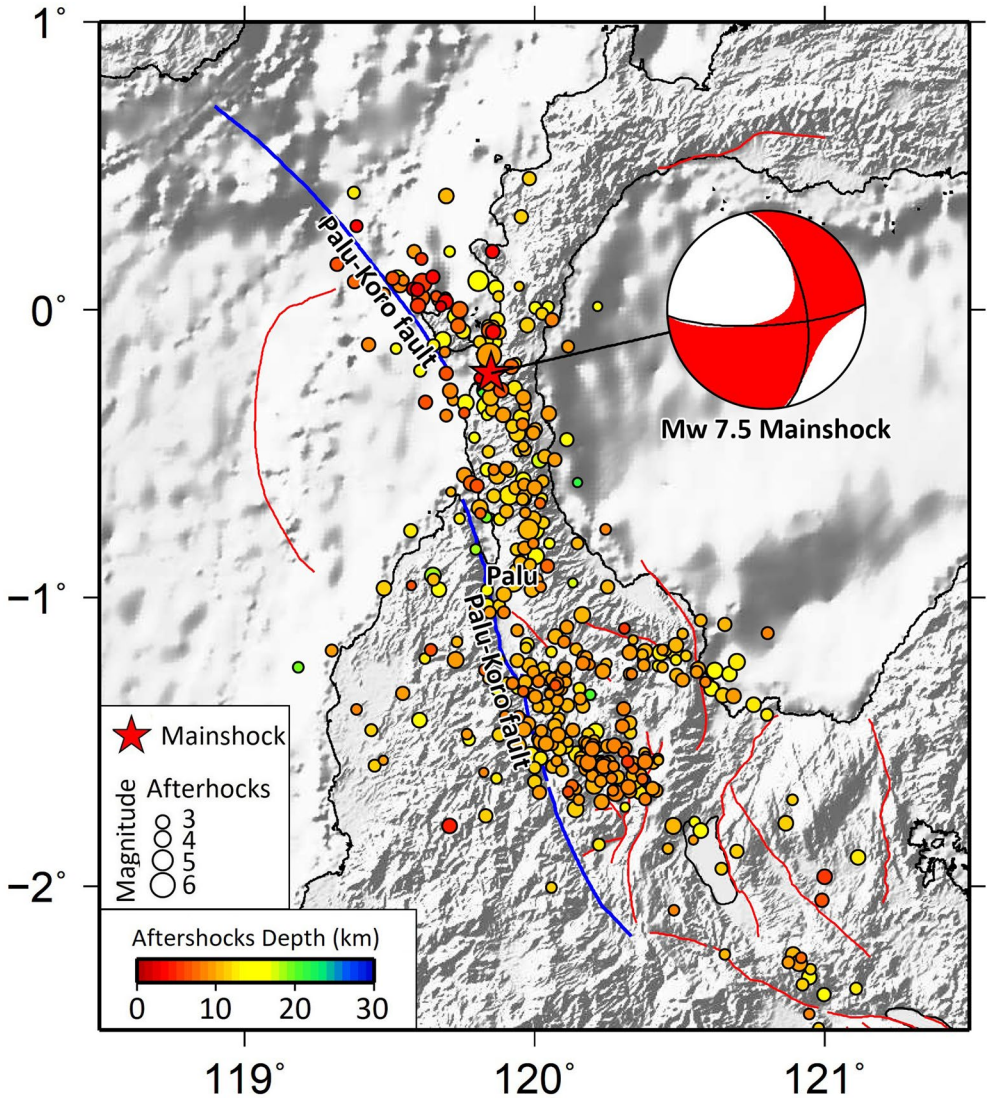

Fig. 2 Map view for relocated events of the Palu aftershocks; red-to-blue circles represent the epicenters of earthquakes as a function of the focal depths. Red star illustrates the epicenter of the mainshock, red beach ball diagram denotes the global centroid moment tensor (gCMT) solution, blue traces correspond to the Palu-Koro Fault and red traces represent other major crustal faults in the region extracted from Irsyam et al. (2017)

the Mw 7.5 mainshock and the swarm earthquakes in Mamasa (Fig. 9).

As noted from the spatiotemporal distribution of the relocated seismicity, the swarm earthquakes in the Mamasa area are not related to the devastating Palu earthquake. Figure 9 indicates that the Mamasa swarm earthquakes occurred approximately 30 days after the larger magnitude ($M > 3$) aftershocks had stopped. Furthermore, it seems very unlikely that a direct dynamic triggering would respond from such a large distance (~ 230 km) (O'Malley et al. 2018) and the timing is beyond the timescale of the dynamic stress transfer. The evidence of a large earthquake triggering other earthquake sequences only occurs at a magnitude of $M > 8$ and is very rare (Johnson et al. 2015). However, the static stress triggering may have contributed

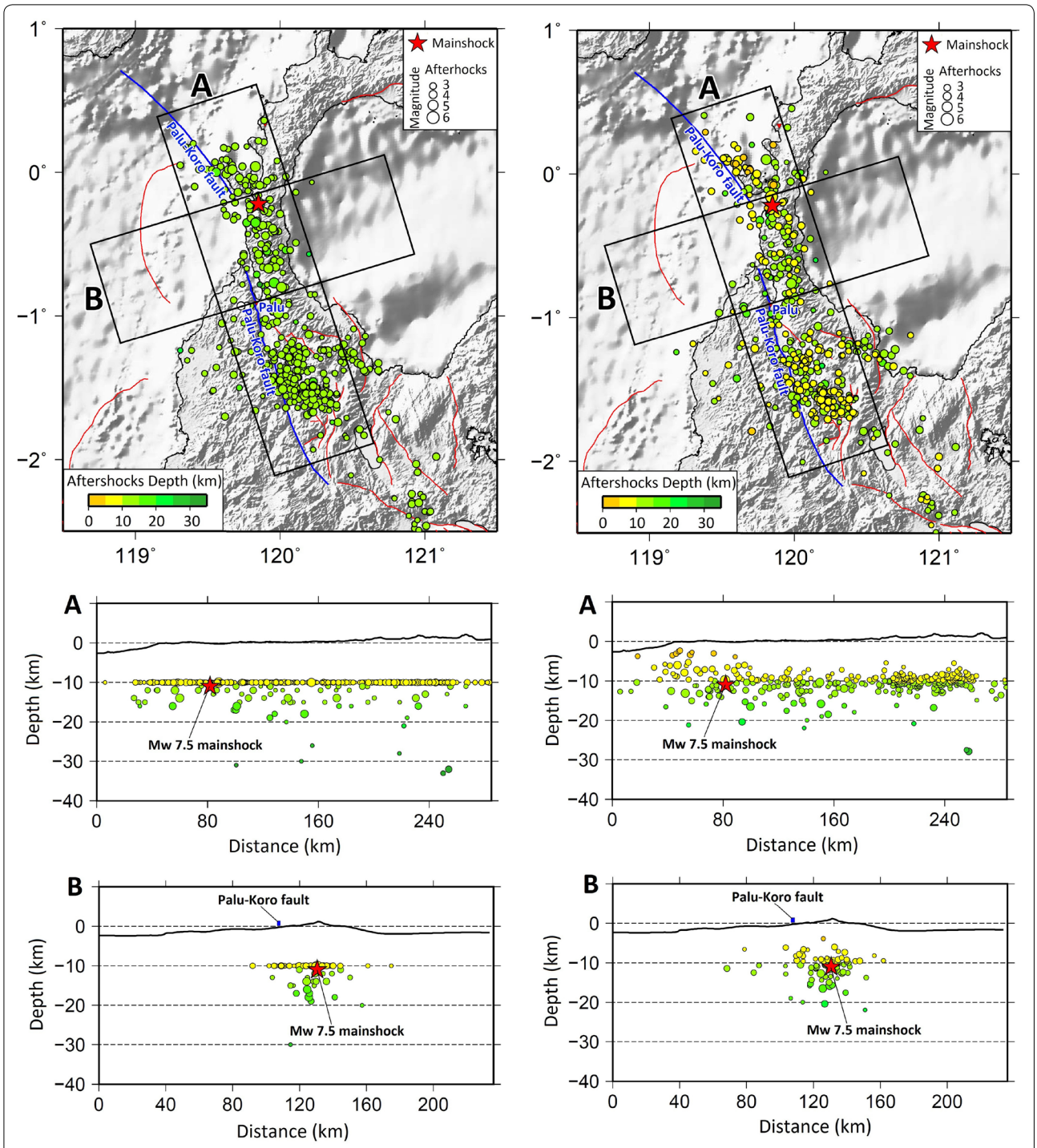

Fig. 3 Vertical cross section of the aftershocks parallel to the fault before relocation (left panel); after relocation (right panel), 386 events, respectively. The red star represents the Mw 7.5 mainshock, and the blue line depicts the Palu-Koro Fault

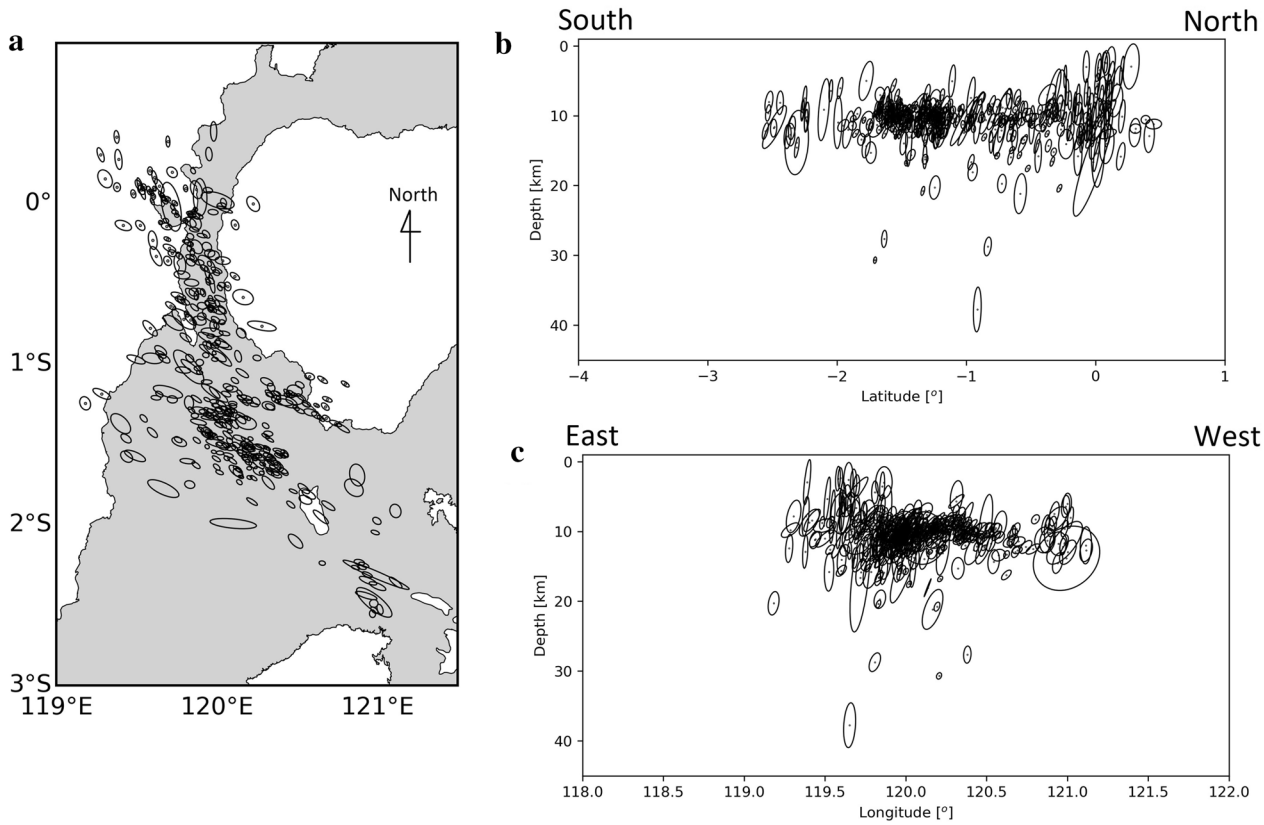

Fig. 4 **a** Map view of relative location errors for the 386 aftershocks along the Palu-Koro Fault Zone; **b** depth view along latitude; and **c** depth view along longitude. Relative horizontal and vertical error ellipses are shown at the 95% confidence level. Ellipses are computed from the major axes of the horizontal and vertical projection of the 95% confidence ellipsoids obtained from a bootstrap analysis of the final double-difference vector

Table 1 Horizontal (DX, DY) and vertical (DZ) deviation shift with Gaussian noise (0.1 s) for the Palu aftershocks

	DX [km]		DY [km]		DZ [km]	
	Mean	**Max**	**Mean**	**Max**	**Mean**	**Max**
Relocated noise (0.1 s)	1.80	12.43	1.18	8.61	0.61	3.88

to the stress accumulation at the Mamasa earthquake sequence. Therefore, a more rigorous study of static stress change, incorporating the area of the Mamasa earthquake sequence, needs to be performed.

Conclusions

We have conducted hypocenter relocations of the aftershocks of the Mw 7.5 earthquake in Palu since the September 28, 2018 event. Our results show that the aftershocks were located to the east of the Palu-Koro

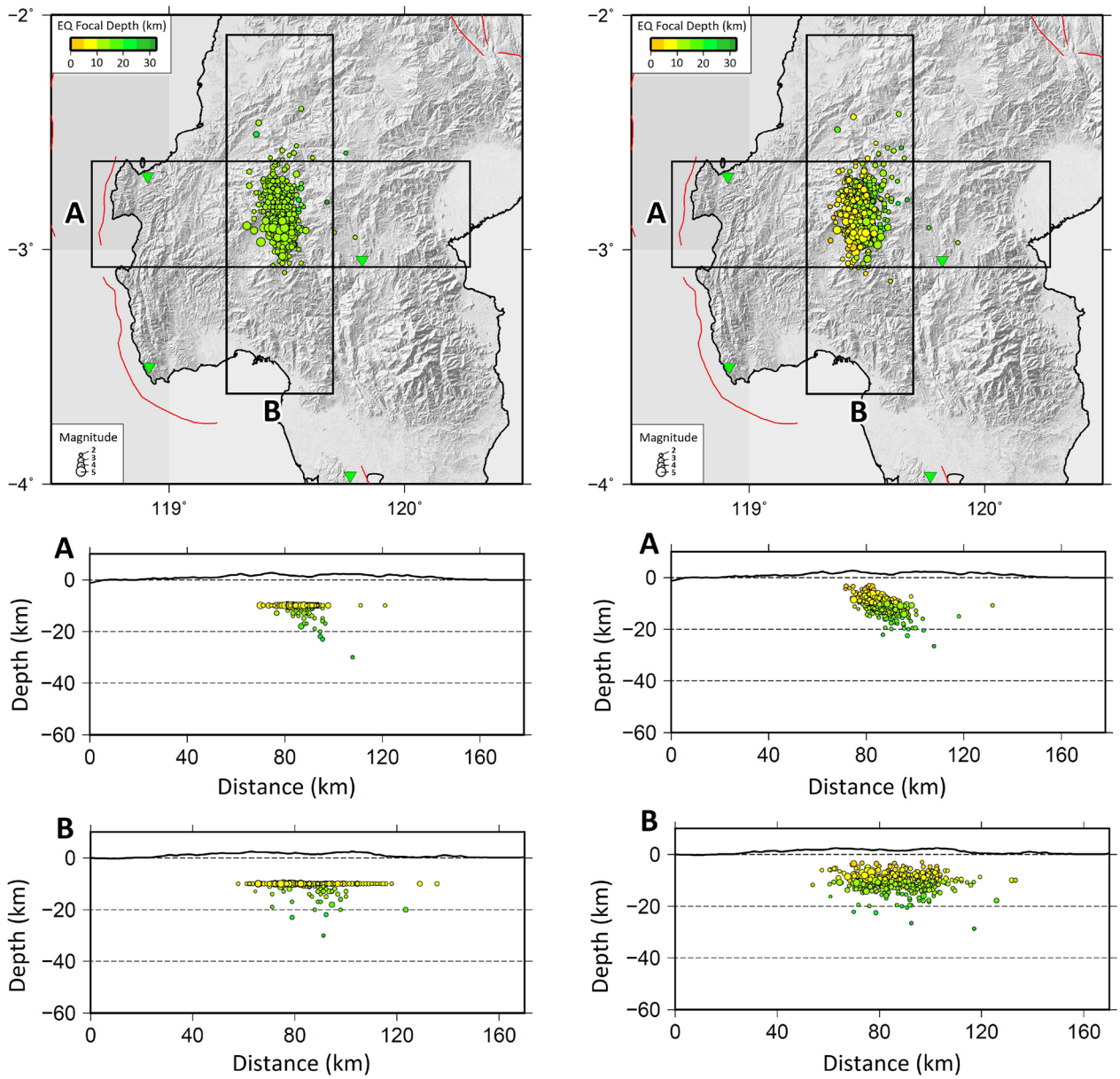

Fig. 5 Map of 535 relocated swarm earthquakes in Mamasa, West Sulawesi; for (left panel) the initial location of the BMKG catalogue; (right panel) after relocation using the double-difference method used in this study

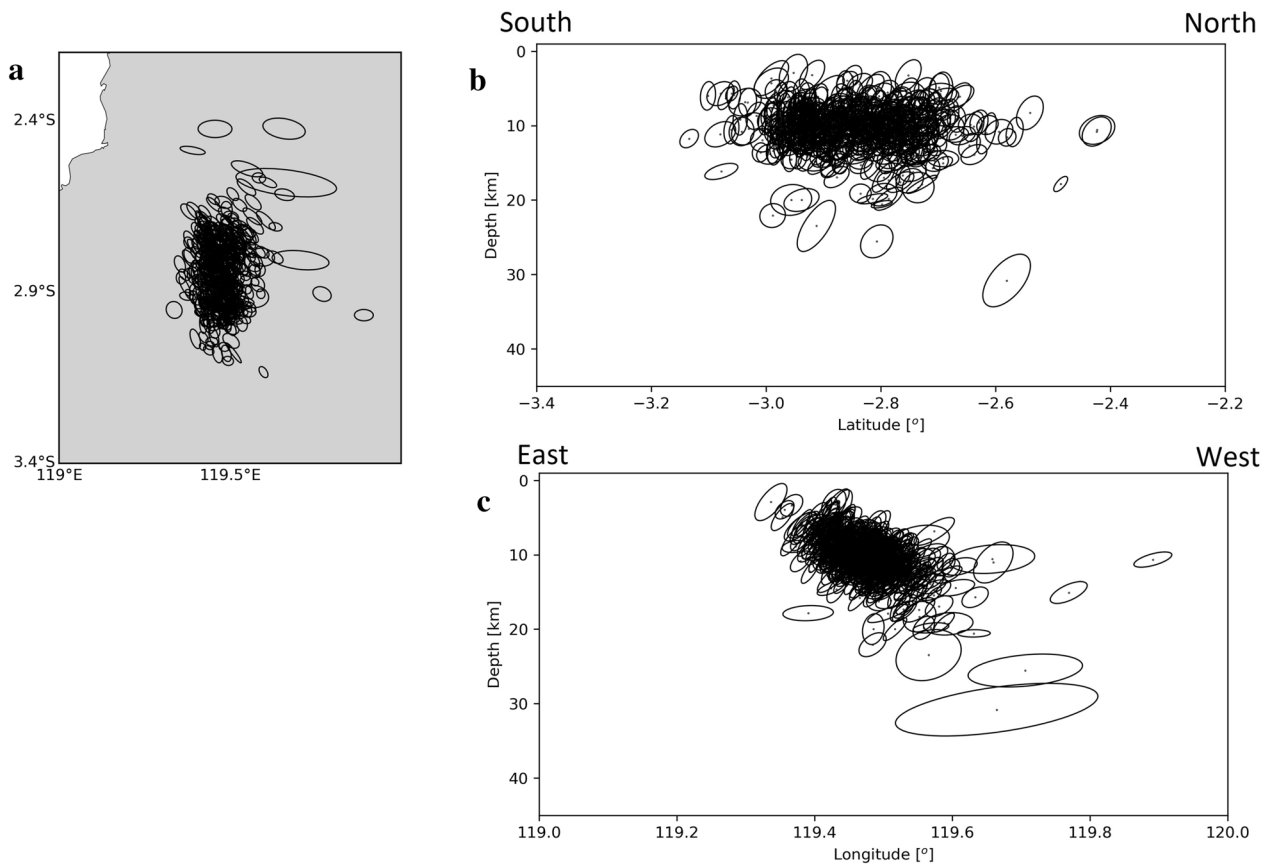

Fig. 6 **a** Map view of relative location errors for the 535 earthquakes in Mamasa; **b** depth view along latitude; **c** depth view along longitude. Relative horizontal and vertical error ellipses are shown at the 95% confidence level. Ellipses are computed from the major axes of the horizontal and vertical projection of the 95% confidence ellipsoids obtained from a bootstrap analysis of the final double-difference vector

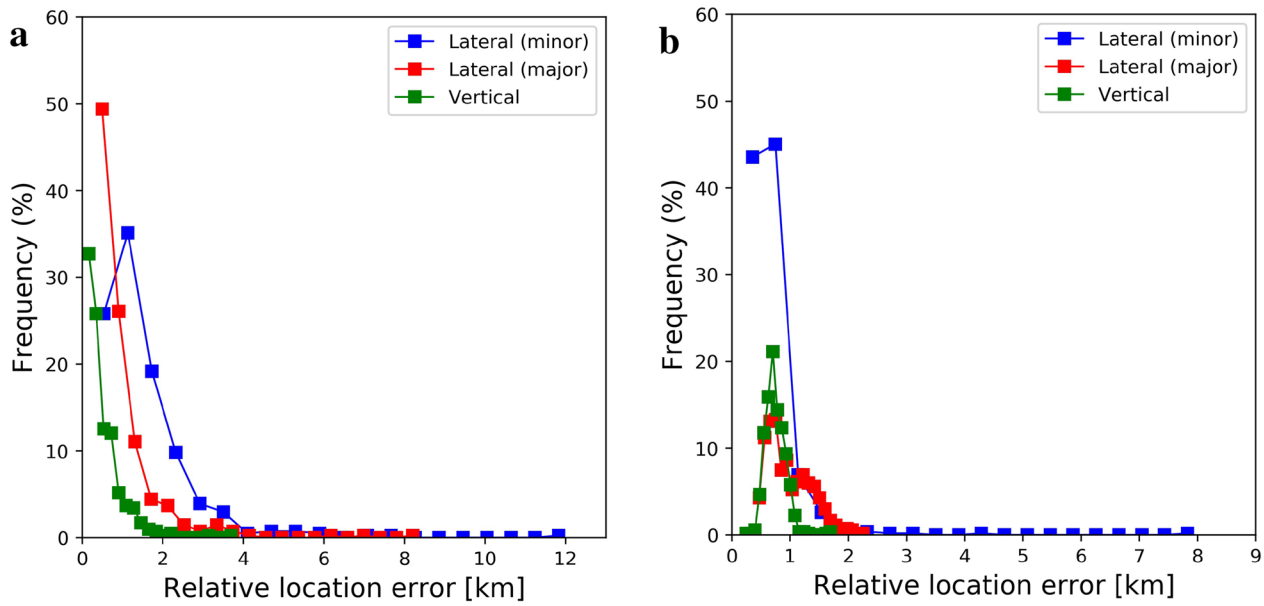

Fig. 7 Histograms of lateral and vertical relative location errors of double-difference solutions for **a** the Palu aftershocks; **b** the Mamasa swarm earthquakes. Errors are computed from the major axes of the horizontal and vertical projection of the 95% confidence ellipsoids obtained from a bootstrap analysis of the final double-difference vector based on 1000 samples with replacement

Table 2 Horizontal (DX, DY) and vertical (DZ) deviation shift with Gaussian noise (0.1 s) for the Mamasa sequence

	DX [km]		DY [km]		DZ [km]	
	Mean	Max	Mean	Max	Mean	Max
Relocated noise (0.1 s)	0.87	8.22	1.03	2.35	0.78	1.77

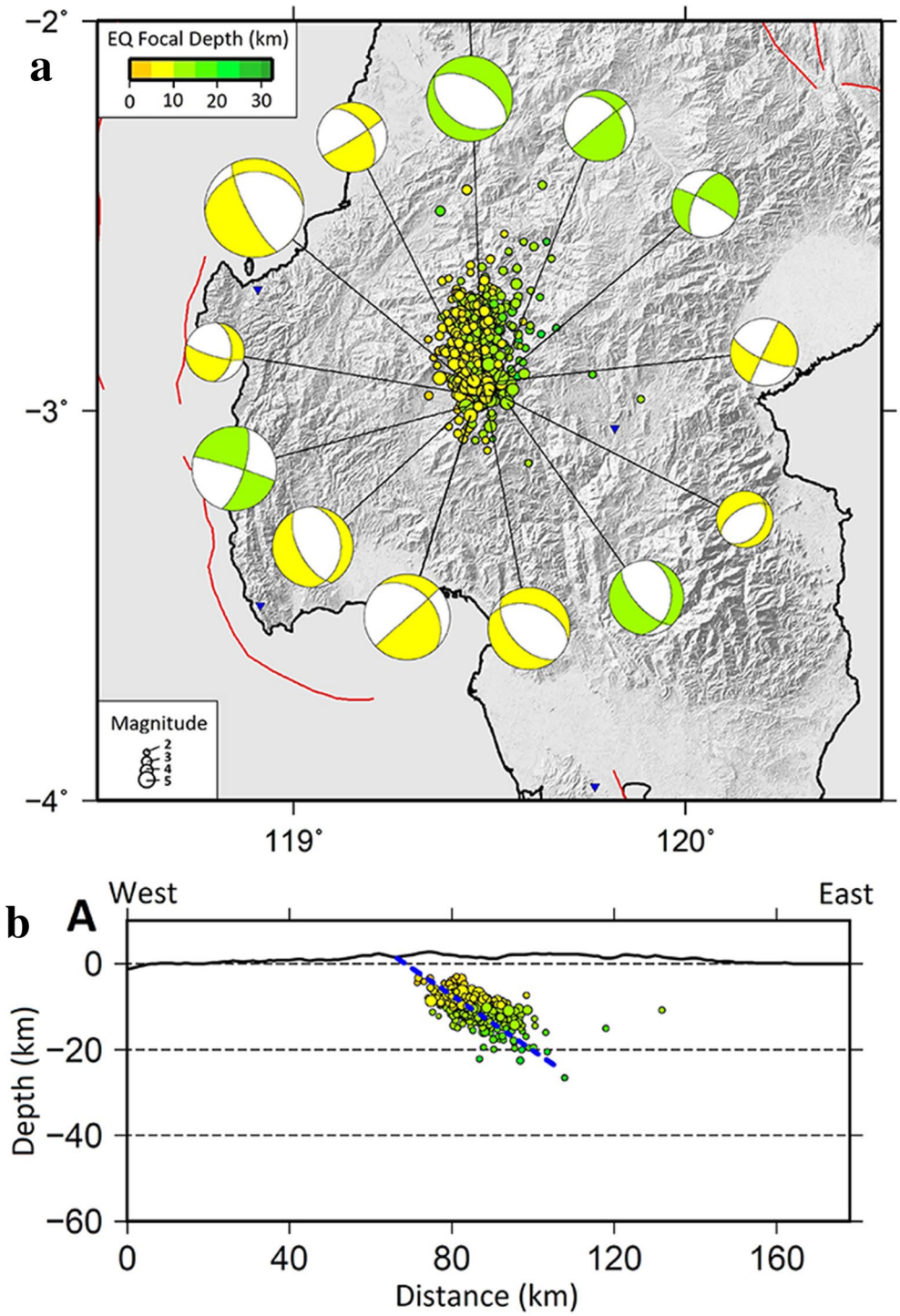

Fig. 8 **a** Focal mechanism solution for selected events ($M > 4.5$) Mamasa swarm earthquakes; **b** cross section A after relocation; dashed blue line is the first-order interpretation of dipping fault, cross section location in Fig. 4

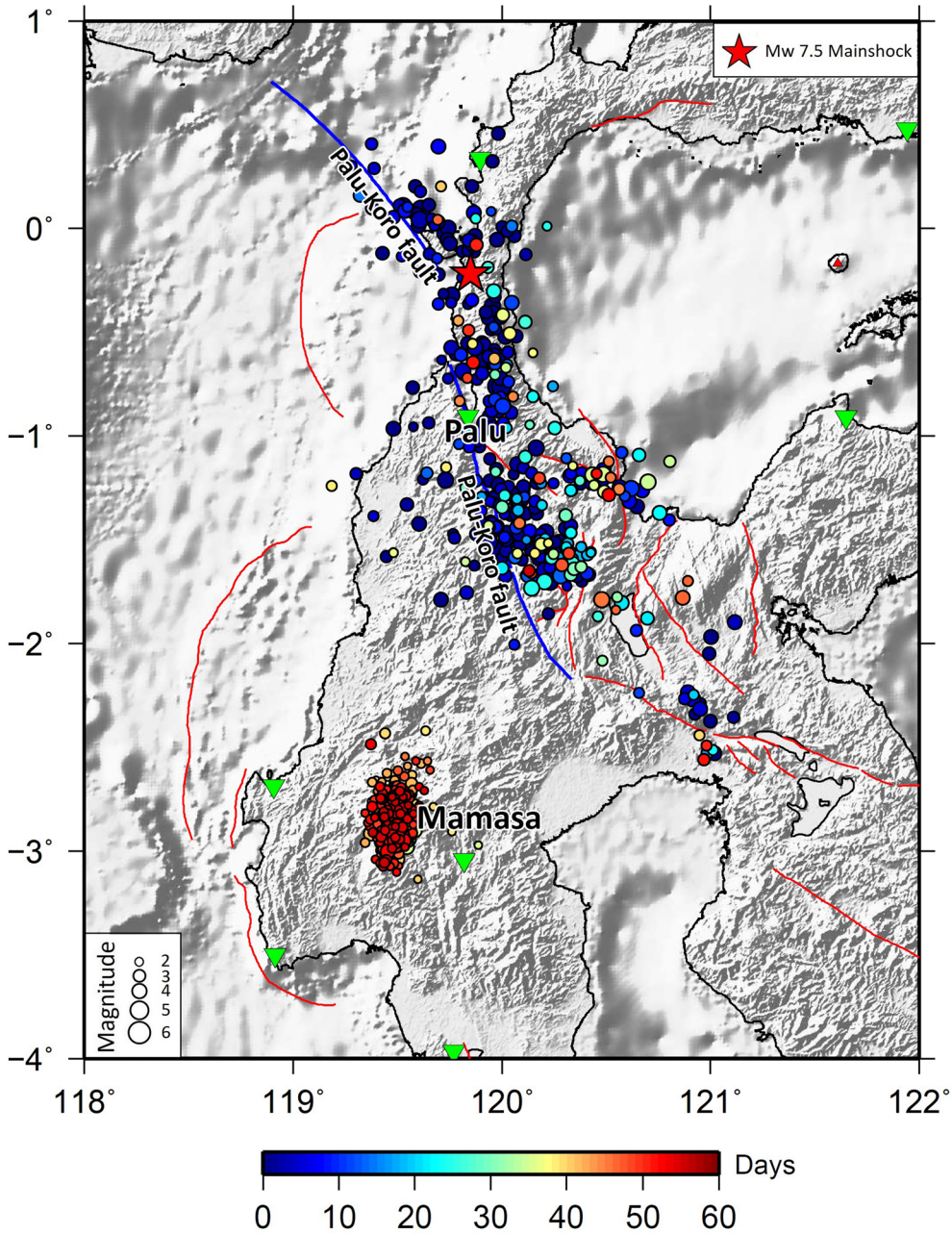

Fig. 9 Map view of spatiotemporal distribution of relocated Palu aftershocks and the Mamasa swarm earthquakes. Colored dots depict the sequence number of events (days) relative to the Mw 7.5 Palu earthquake (September 28, 2018, to November 22, 2018)

Fault Line, and these results are consistent with the deformation data of the area. The relocated swarm earthquakes in Mamasa most likely correspond to the activity of the local fault (dipping at a ~ 45° angle) and extend from north to south for a length of ~ 50 km.

Supplementary information

Supplementary information accompanies this paper at https://doi.org/10.1186/s40562-019-0148-9.

Additional file 1. The relocated earthquake catalog for aftershocks of the Mw 7.5 Palu earthquake and swarm earthquakes of Mamasa from September 28 to November 22, 2018.

Acknowledgements
We are grateful to the Indonesian Agency for Meteorology, Climatology, and Geophysics (BMKG) for access to their earthquake data which were used in this study. All figures were made using Generic Mapping Tools (Wessel and Smith 1998). We thank James D. P. Moore for constructive comments, which helped us improve the manuscript considerably.

Authors' contributions
PS, ADN, SW, CIA, NTP, KHP, DD, SHW conceived the study. PS, ADN, SW, KHP contributed to the writing of the manuscript. All authors contributed to the preparation of the manuscript. All authors read and approved the final manuscript.

Funding
This study was supported in part by the Indonesian Directorate General of Higher Education (DIKTI) research funding 2018–2019, awarded to S.W., and research funding from the Institut Teknologi Bandung (ITB) 2018, awarded to A.D.N.

Availability of data and materials
The relocated earthquake catalog data are available in Additional file 1.

Competing interests
The authors declare that they have no competing interests.

Author details
[1] Geophysical Engineering Study Program, Faculty of Mining and Petroleum Engineering, Institut Teknologi Bandung, Bandung 40132, Indonesia. [2] Agency for Meteorology, Climatology, and Geophysics (BMKG), Bandung 40161, Indonesia. [3] Global Geophysics Research Group, Faculty of Mining and Petroleum Engineering, Institut Teknologi Bandung, Bandung 40132, Indonesia. [4] Center for Earthquake Science and Technology, Institut Teknologi Bandung, Bandung 40132, Indonesia. [5] Geodynamic and Sedimentology Research Group, Faculty of Earth Sciences and Technology, Institut Teknologi Bandung, Bandung 40132, Indonesia. [6] Physical Science and Engineering, King Abdullah University of Science and Technology, Thuwal, Saudi Arabia. [7] Agency for Meteorology, Climatology, and Geophysics (BMKG), Jakarta 10610, Indonesia.

Received: 20 August 2019 Accepted: 3 December 2019
Published online: 16 December 2019

References

Bao H, Ampuero J-P, Meng L, Fielding EJ, Liang C, Milliner CWD, Fen T, Huang H (2019) Early and persistent supershear rupture of the 2018 magnitude 7.5 Palu earthquake. Nat Geosci 12:200–205. https://doi.org/10.1038/s41561-018-0297-z

Billings SD (1994) Simulated annealing for earthquake location. Geophys J Int 118:680–692. https://doi.org/10.1111/j.1365-246X.1994.tb03993.x

Daryono MR (2016) Paleoseismology tropis Indonesia (dengan studi kasus di Sesar Sumatra, Sesar Palukoro-Matano, dan Sesar Lembang). Phd thesis, Institut Teknologi Bandung (in Indonesia)

Efron B (1982) The Jackknife, the bootstrap and other resampling plans. Society for Industrial and Applied Mathematics, Philadelphia. https://doi.org/10.1137/1.9781611970319

Gusman AR, Supendi P, Nugraha AD, Power W, Latief H, Sunendar H, Widiyantoro S, Daryono, Wiyono SH, Hakim A, Muhari A, Wang X, Burbidge D, Palgunadi K, Hamling I, Daryono MD (2019) Source model for the tsunami inside Palu Bay following the 2018 Palu earthquake, Indonesia. Geophys Res Lett. https://doi.org/10.1029/2019GL082717

Irsyam M, Widiyantoro S, Natawidjaya DH, Meilano I, Rudyanto A, Hidayati S, Triyoso W, Hanifa NR, Djarwadi D, Faizal L, Sunarjito (2017) Peta sumber dan bahaya gempa Indonesia tahun 2017. Pusat Penelitian dan Pengembangan Perumahan dan Permukiman, Kementerian Pekerjaan Umum dan Perumahan Rakyat (in Indonesian)

Ismullah MF, Nugraha AD, Ramdhan M, Wandono (2017) Precise hypocenter determination around Palu Koro fault: a preliminary results. In: IOP conference series: earth and environmental science, pp 012056

Johnson CW, Bürgmann R, Pollitz FF (2015) Rare dynamic triggering of remote $M \geq 5.5$ earthquakes from global catalog analysis. J Geophys Res Solid Earth 120:1748–1761. https://doi.org/10.1002/2014JB011788

Kennett BLN, Engdahl ER (1991) Traveltimes for global earthquake location and phase identification. Geophys J Int 105:429–465. https://doi.org/10.1111/j.1365-246X.1991.tb06724.x

Kennett BLN, Engdahl ER, Buland R (1995) Constraints on seismic velocities in the earth from traveltimes. Geophys J Int 122:108–124. https://doi.org/10.1111/j.1365-246X.1995.tb03540.x

Nugraha AD, Supendi P, Widiyantoro S, Daryono, Wiyono SH (2018a) Earthquake swarm analysis around Bekancan area, North Sumatra, Indonesia using the BMKG network data: Time periods of February 29, 2015 to July 10, 2017. In: AIP conference proceedings, pp 020092. https://doi.org/10.1063/1.5047377

Nugraha AD, Supendi P, Widiyantoro S, Daryono, Wiyono SH (2018b) Hypocenter relocation of earthquake swarm around Jailolo volcano, North Molucca, Indonesia using the BMKG network data: time periods of September 27-October 10, 2017. In: AIP conference proceedings. https://doi.org/10.1063/1.5047378

O'Malley RT, Mondal D, Goldfinger C, Behrenfeld MJ (2018) Evidence of systematic triggering at teleseismic distances following large earthquakes. Sci Rep 8:11611. https://doi.org/10.1038/s41598-018-30019-2

Pramono S, Prakoso W, Rahayu A, Cummins P, Rahayu A, Rudyanto A, Syukur F, Sofian (2017) Investigation of subsurface characteristics by using a Vs30 parameter and a combination of the Hvsr and Spac methods for microtremor arrays. Int J Technol 8:983. https://doi.org/10.14716/ijtech.v8i6.682

Shearer PM (1997) Improving local earthquake locations using the L1 norm and waveform cross correlation: application to the Whittier Narrows, California, aftershock sequence. J Geophys Res 102:8269–8283. https://doi.org/10.1029/96JB03228

Socquet A, Simons W, Vigny C, McCaffrey R, Subarya C, Sarsito D, Ambrosius B, Spakman W (2006) Microblock rotations and fault coupling in SE Asia triple junction (Sulawesi, Indonesia) from GPS and earthquake slip vector data. J Geophys Res. https://doi.org/10.1029/2005JB003963

Socquet A, Hollingsworth J, Pathier E, Bouchon M (2019) Evidence of supershear during the 2018 magnitude 7.5 Palu earthquake from space geodesy. Nat Geosci 12:192–199. https://doi.org/10.1038/s41561-018-0296-0

Sokos EN, Zahradnik J (2008) ISOLA a Fortran code and a Matlab GUI to perform multiple-point source inversion of seismic data. Comput Geosci 34:967–977. https://doi.org/10.1016/j.cageo.2007.07.005

Supendi P, Nugraha AD, Puspito NT, Widiyantoro S, Daryono, Wiyono SH (2018a) Identification of active faults in West Java, Indonesia, based on earthquake hypocenter determination, relocation, and focal mechanism analysis. Geosci Lett. https://doi.org/10.1186/s40562-018-0130-y

Supendi P, Nugraha AD, Widiyantoro S (2018b) Hypocenter relocation of the aftershocks of the Poso, Sulawesi (Mw 6.6, May 29, 2017) event using the BMKG network data. In: AIP conference proceedings, pp 020076. https://doi.org/10.1063/1.5047361

Utama MRJ, Nugraha AD, Puspito NT (2015) Seismicity studies at Moluccas area based on the result of hypocenter relocation using HypoDD. In: AIP conference proceedings, pp 030022. https://doi.org/10.1063/1.4915030

Waldhauser F (2001) hypoDD-A program to compute double-difference hypocenter locations, USGS open file report 2001-113

Waldhauser F, Ellsworth WL (2000) A double-difference earthquake location algorithm: method and application to the northern Hayward Fault, California. Bull Seismol Soc Am 90:1353–1368. https://doi.org/10.1785/0120000006

Watkinson IM (2011) Ductile flow in the metamorphic rocks of central Sulawesi. Geol Soc Lond Spec Publ 355:157–176. https://doi.org/10.1144/SP355.8

Wessel P, Smith WHF (1998) New, improved version of generic mapping tools released. Eos Trans Am Geophys Union 79:579. https://doi.org/10.1029/98EO00426

Publisher's Note